International Journal of Pharmacy and Pharmaceutical Sciences

Print ISSN: 2656-0097 | Online ISSN: 0975-1491 Vol 14, Issue 1, 2022

Original Article

OPTIMIZATION OF RIVASTIGMINE CHITOSAN NANOPARTICLES FOR NEURODEGENERATIVE ALZHEIMER; *IN VITRO* AND *EX VIVO* CHARACTERIZATIONS

MONA IBRAHIM El-ASSAL*, DALIA SAMUEL

Department of Pharmaceutics and Pharmaceutical Technology, Faculty of Pharmacy, Future University in Egypt, 11835, Cairo, Egypt
Email: mona.ibrahim@fue.edu.eg

Received: 16 Sep 2021, Revised and Accepted: 10 Nov 2021

ABSTRACT

Objective: In an attempt to optimize the anti-Alzheimer effect, rivastigmine-loaded chitosan nanoparticles were developed in order to target of brain through skin permeation.

Methods: Rivastigmine-loaded chitosan-tripolyphosphate nanoparticles were prepared by modified ionic gelation method using tween 80 surfactants in different batches with variable chitosan/cross-linker ratios, desirability factors were applied to choose the optimal Nanocarrier and (F15) was selected. Different rivastigmine concentrations were loaded and the highest encapsulation efficiency formulae chosen for further study and evaluated by scanning electron microscopy (SEM), transmission electron microscopy (TEM) and differential scanning calorimetric (DSC). Further, drug loading, *Ex-vivo* skin permeation of Nano-gel, and kinetic studies were carried out in addition to stability along three months under different temperature.

Results: Particle size and polydispersity index showed average 291.6±7.70 to 490.6±7.42 d. nm. and 0.333±0.04 to 0.570±0.023 respectively. The nanoparticles were spherical in shape. Drug concentrations 4% w/w showed the highest drug entrapment efficiency (89.80%) and drug loading (40.81). *Ex vivo* studies shows that gel formulae of rivastigmine loaded chitosan nanoparticles was not irritant to rat skin had better skin permeation than chitosan nanoparticles aqueous dispersion also capable of releasing the drug in a sustained manner, and follow kinetic diffusion model. Optimum formula F15 was physical and chemical stable.

Conclusion: The experimental results showed the suitability of chitosan nanoparticles coated with a surfactant as a potential carrier for permeation through skin and brain, providing sustained delivery of rivastigmine.

Keywords: Chitosan, Ionotropic gelation, Polymeric nanoparticles, Rivastigmine, Alzheimer disease

DOI: https://dx.doi.org/10.22159/ijpps.2022v14i1.43145. Journal homepage: https://innovareacademics.in/journals/index.php/ijpps.

INTRODUCTION

Drug delivery to the central nervous system is a major menace as multiple cerebral diseases like Alzheimer's, brain tumors, prion diseases are cropping up nowadays. The blood-brain barrier (BBB) represents an insurmountable obstacle for a large number of central nervous system (CNS) active drugs [1-3]. Currently, nanoparticles are used as drug delivery vehicles to deliver such drugs to the brain by infiltrating BBB and these may provide a significant strategy to break this impasse [1, 3]. These drug delivery systems offer numerous advantages over conventional dosage forms, including improved efficacy, reduced toxicity and improved patient compliance. Nanoparticles can also be utilized in the form of carriers in drug delivery [4, 5].

Nanostructure-mediated drug delivery enhances drug bioavailability, improves the timed release of drug molecules, and enables precision drug targeting [6, 7]. They also decrease the excessive and unfavorable biodistribution of the drug. This leads to delayed drug clearance and retarded drug metabolism, resulting in their prolonged release pattern [8].

Depending on the method of preparation, Nanoparticles, Nanospheres, or Nanocapsules can be tailored for different properties and release characteristics for the best delivery or encapsulation of the therapeutic agent, cross BBB entrapping the original characteristics of the therapeutic drug molecule [9]. Furthermore, this system may reduce drug leaching in the brain and decrease peripheral toxicity [10-12].

Chitosan is a biocompatible, bioactive, and biodegradable polymer that can be easily engineered. Because of its cationic charge, biocompatibility and low toxicity, chitosan has been used as a vehicle system for the delivery of genes, proteins (including antibodies) and various categories of drugs [13]. Chitosan was recognized of its mucoadhesive and good biodegradability properties affect its bioactivity on the blood-brain barrier at the molecular level, which is advantageous in therapies for neurological disorders.

Rivastigmine is an anticholinesterase agent having favorable efficacy and safety in patients with Alzheimer type dementia and has been widely used for the treatment of mild to moderate Alzheimer's disease [14, 15] and recently in Parkinson's disease [16, 17]. Orally administered rivastigmine has a short half-life of 1.5 h due to hepatic first-pass metabolism [17].

MATERIALS AND METHODS

Materials

Rivastigmine (purity 98.9%) was kindly gifted by Mach Premiere Pharmaceutical Industries in Cairo, Egypt. Chitosan (degree of DE acetylation of 93%), sodium tri-polyphosphate (STPP) and both carbopol and triethanolamine were purchased from (Sigma-Aldrich St. Louis, MA, USA). Sodium hydroxide, Methyl alcohol, ethyl alcohol, glacial acetic acid and tween 80 were purchased from El-Nasr Company for chemicals (Cairo, Egypt). Disodium hydrogen phosphate, sodium dihydrogen phosphate, potassium chloride, sodium chloride was purchased from El Shark El Oust Chemical trade company (Cairo, Egypt). Water used all over the study was double distilled and of high purity. All other chemicals used are analytical grade and were used without further purification.

Methods

Preparation of chitosan nanoparticles by modified ionotropic gelation method

Chitosan nanoparticles were prepared using ionotropic gelation of chitosan with sodium tripolyphosphate STPP anions [18] with some

modification. Chitosan was dissolved in purified water at various ratios 0.5% w/v, 0.7% w/v, 1% w/v, 1.2% w/v and 1.4% w/v. STPP was also dissolved in purified water at various concentrations of 0.6% w/v, 0.8% w/v, 1% w/v, 1.2% w/v and 1.4% w/v. Each ratio of chitosan was dissolved in an aqueous solution containing 1% (v/v) glacial acetic acid and leaving it under high stirring (1400 r/min) for 2 h. The pH was adjusted to pH 5 with 0.1N NaOH. Tween 80 was added as a modified ingredient with a constant ratio 0.2 ml. STPP as a physical cross-linker was dissolved separately in deionized water and added to the chitosan solution as drops at a high rate under vigorous magnetic stirring at room temperature (25 °C) [19]. Nanoparticles formed spontaneously under mechanical stirring; the resulting aqueous dispersion was then homogenized (Heidolph, PH-E3.7-HGZI, Germany) at 22000 r/min for 3 min and left under ultra-sonication for 45 min. Different formulae were prepared with different STPP: chitosan ratios.

Desirability factor excel sheet was used, plain nanoparticles formulae data were applied to choose the optimal formula depending on the smallest particle size, the lowest PDI and the highest zeta potential.

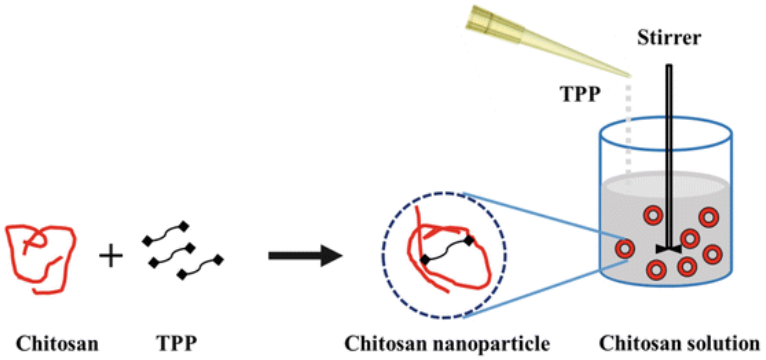

Fig. 1: Diagram for ionic gelation technique

Preparation of rivastigmine-loaded chitosan nanoparticles

Rivastigmine (RS) was loaded in an optimized chitosan nanoparticles carrier. RS different concentrations (o.5 %w/v, 1 %w/v, 2 %w/v, 3 %w/v and 4 %w/v) were added to chitosan dissolved in acetic acid aqueous solution after 1 h of high stirring rate. Tween 80 was added and RS-loaded CSNPs colloidal dispersion were formed spontaneously upon rapid addition of an aqueous drop of cross-linker STPP under high stirring rate followed by homogenization for 3 min at 22,000 r/min and sonication for 45 min. Gel of RS-CSNPs prepared using carbopol and triethanolamine.

***In vitro* evaluation parameters of optimized loaded RS-CSNPs**

Differential scanning calorimetric (DSC)

DSC interactions are typically ascertained as the elimination of endothermic peaks, appearance of recent peaks, the difference in peak height and its onset, peak temperature/melting points and relative peak area, or enthalpy. It likewise gives data regarding drug excipient compatibility and the development of a new substance. Thermal analysis was used in order to elucidate any interactions between rivastigmine, investigated polymer and the cross-linking agent. DSC was carried out using Shimadzu, DSC 60 thermal analyzer with a liquid nitrogen cooling accessory. The analysis was performed under purge of dry nitrogen gas (40 ml/min^{-1}). A sample of 2–5 mg was placed in an aluminum crucible cell and was firmly crimped with the lid to provide an adequate seal. The samples were heated from ambient temperature to 400 °C at a preprogrammed heating rate of 10 °C/min^{-1}. All samples were analyzed in the same manner i.e. pure powders, physical mixture or dry formulae.

Optical micrograph

A thin layer of a formed colloidal dispersion of loaded RS-CSNPs were spread on a slide, diluted with a small drop of deionized water then dried. The nature of nanoparticles was observed and the presences of drug-loaded nanoparticles, which are insoluble, were focused under the light microscope (Olympus-CKX 41 SF, Philippines) at high magnification powers (10×and40×). Photomicrographs were taken using Fujifilm Finepix F 40 fd (8.3 MP) digital camera with 3 × optical zoom [20].

Determination of particle size, PDI and zeta potential

Particle size measurements of plain and drug-loaded CSNPs were determined using Malvern Zeta Seizer by dynamic light scattering (Nano ZS, Malvern, and Worcester-shire, UK). Before measurements samples were diluted with distilled water (1:10 ratio) and measured in triplicate at 25 °C. The ionic potential at the particles surface called Zeta potential. It is a logical term for electrokinetic potential in colloidal dispersions and the most imperative parameter for physical stability of nanoparticles. The higher the electrostatic repulsion between the particles more is the stability [21]. Before measurement, samples were dispersed in distilled water. Three replicates were measured.

Transmission electron microscope (TEM)

The morphology and size of the prepared CSNPs, either plain or drug-loaded formulations, were investigated by TEM (HU-12A, Hitachi Ltd, Mito, Japan). A drop of the dispersion was diluted 10-fold using deionized water, and then a drop of the diluted dispersion was applied to a carbon-coated 300 mesh copper grid and left for 1 min to allow some of the CSNPs to adhere to the carbon substrate. The remaining dispersion was removed by absorbing the drop with the corner of a piece of filter paper. After twice rinsing the grid with deionized water for (3–5 s) a drop of 2% aqueous solution of uranyl acetate was applied for 1 s. The remaining solution was removed by absorbing the liquid with the tip of a piece of filter paper and the sample was air-dried [22].

Scanning electron microscope

Scanning electron microscopy (SEM) (Hitachi-S 3400N) was used to study visualization that provides surface morphology and basic composition of the sample by emitting electrons [23]. The sample previously dried by lyophilizes using freeze dryer (Christ, Alpha2-4LD Plus, Harz, Germany) was mounted directly onto the SEM using double-sided sticking tape and was gold spray-coated [24].

Determination of entrapment efficiency percent EE%

The un-entrapped drug in loaded CSNPs formulation can be separated by using centrifugation method in which a specific amount of nanoparticles dispersion is subjected to cold centrifuge (4 °C) at a specific speed 15,000 r/min for 30 min (Sigma,3-30KS, Germany). Then remove the supernatant liquid and an assay of free drug determined after certain dilution by measuring the absorbance at λ max 263 nm by using UV-spectrophotometer (Shimadzu-UV/800, Japan), followed by application in pre-determined water calibration curve equation. The EE% and drug loading calculated from the following equations:

$$\text{Entrapment efficiency (\%)} = \left[\frac{\text{Total entrapped drug} - \text{Unentrapped drug}}{\text{Total entrapped drug}}\right] \times 100$$

$$\text{Drug loading (\%)} = \left[\frac{\text{Amount of drug in nanoparticles}}{\text{Mass of nanoparticles}}\right] \times 100$$

Drug content

It is determined by weighing the equivalent amount of dried lyophilized preparation of loaded optimum formula and placed in 20 ml phosphate-buffered saline pH 7.4, followed by agitation in an incubator shaker (160 r/min) for 24 h at 37 °C. The solution filtered through what man filter 42 pore size and after suitable dilution drug solubilized was analyzed spectrophotometrically at λ max 207 nm, followed by application in pre-determined phosphate buffer calibration curve equation.

Rheological measurements

Rheology's of CSNPs gel loaded with RS was performed with a cone and plate rheometer (Anton Paar®GmbH, Ostfildern, Germany). Up and down portions of the flow curves were determined using parallel plate geometry (50 mm diameter), where, the gap between the two plates was 1 mm. About 0.5 g of the tested formulation was applied to the plate and left until the temperature of the plate reached 25±1 °C. The measurements were made over the range from 10, 15, 20, 25, 50, and 75 up to 250 r/min with 20 s between each two successive speeds. The rheological behavior was evaluated by plotting the shear stress versus the obtained shear rate values. The flow behavior was studied according to Farrow's equation [25].

$$\text{Log D} = \text{N Log S} - \text{Log } \dot{\eta}$$

Where D is the shear rate (s^{-1}), S is the shear stress (Pa), N is Farrow's constant and $\dot{\eta}$ is the viscosity (Pa . s). N is the slope of the plot of log D against log S, which indicates the deviation from Newtonian flow. When N is less than one, it indicates dilatant flow (shear rate thickening). If N is greater than one, it indicates pseudo plastic or plastic flow (shear rate thinning). When the system showed thixotropic behavior, the hysteresis area (H. A.) between the upward and a downward curve was measured, adopting the trapezoidal rule.

***Ex-vivo* studies**

Skin irritancy test

An Irritancy test was carried out to determine the possible localized reaction of the selected formula on the skin since skin safety is of prior consideration for transdermal delivery systems. A single dose of 1 g of the selected medicated gel formulation contain I mg drug was applied to the left side of the shaved back of six male albino mice (34±0.5 g) and the right side was considered as control. The control area was further divided into two sub areas, one receiving the selected formulation unloaded with the drug (positive control) and the other receiving no treatment (negative control). The development of erythema was monitored daily for 6 d. Extents of development of erythema were indicated on the basis of the following [26].

0: No erythema development; 2: barely visible few blood vessels and light erythema development; 4: main blood vessels visible and slight erythema development; 6: main blood vessels more obvious and slight erythema development. Irritation potential was calculated using the following equation:

Resultant index = A. B

Number of observation days'

Where A, B are representing erythema value and corresponding day, respectively.

Preparation of full-thickness skin

Male albino mice (12 w old and weighing 34±0.5 g) were obtained from the Central Animal Facility. Methodology was approved by the Faculty Ethics Committee (REC-FOPFUE-15/114). Hairs from the dorsal surface were removed using an animal hair clipper (Sterling 2, Wahl, UK). Animals were euthanized by the use of overdose of sodium thiopental following with full-thickness skin was harvested. The subcutaneous tissue was removed surgically. The skin was washed with phosphate-buffered saline (pH 7.4) [27]. All measurements were carried out in a single ventilated room temperature, ~25 °C; relative humidity, ~38–40%.

Skin permeation experiments

Full-thickness skin was mounted between the two compartments of Franz diffusion cells with the stratum corneum side up and with an effective area of 1.767 cm^2. The receptor compartment capacity (6.8 ml) was then filled with phosphate-buffered saline (pH 7.4) and maintained at 37±0.5 °C with a constant stirring speed of 600 r/min using helix stirrer. The dermal side of the skin which was placed in contact with the receptor compartment fluid was equilibrated for 30 min [28]. Then CSNPs gel in a dose equivalent to 1 mg RS/g gel was evenly spread on the stratum cornium side of the skin in donor compartment and covered with Parafilm (American Can, USA). Aliquots (1 ml) were withdrawn from the receptor compartment at time intervals 1, 2, 4, 8, 12, 16, 18, 20 and 24 h with immediate replacement with fresh medium to maintain the sink conditions constantly and a constant volume as well also calibration curve of rivastigmine in phosphate buffer saline pH 7.4 media was used to calculate drug concentrations. The concentrations of the drug in the withdrawn samples were determined using a spectrophotometer at λ max 204 nm. Data were analyzed by plotting the mean percentage cumulative amount of drug permeated versus time to investigate the best fit to distinct kinetic model to elucidate the drug permeation mechanism. Flux and permeability coefficient were calculated by the following equation

$$J = D\, dc/dx$$

Where D is the diffusion coefficient and is a function of the size, shape and flexibility of the diffusing molecules as well as the membrane resistance. C is the concentration of the diffusion species. X is the spatial coordinate.

Kinetic studies

In order to know the mechanism of drug release from the CSNPs, the experimental release data were fitted on various release model commonly used to describe the release kinetics from nanoparticles such as First order, second order, Higuchi kinetic models, Hixson-Crowell kinetic models, diffusion and Baker model a pH 7.4 using multiple linear regression analysis (sigma plot 11 software). The release rate constant (K) and correlation coefficient (r^2) close to unity was taken as order of release. The following models were fitted: log cumulative % drug remaining versus time (first-order kinetic model), log concentrations plot versus time is a straight line with k equal slope of the line (second-order kinetic model), cumulative % drug release versus square root of time (Higuchi model), cube root of the initial concentration minus cube root of percent remaining versus time (Hixson-Crowell models), the release rate constant *k*, corresponds to the slope and drug release studies were plotted as [d (Mt/M)]/dt with respect to the root of time inverse (Baker Lonsdale) [29].

Stability study for optimizes formulae

Optimum loaded CSNPs were stability studied by keeping the formulas at two different temperature conditions like refrigeration temperature (4±2 °C) and room temperature (25±2 °C) in aluminum foil sealed glass vials. The samples were withdrawn at different time intervals over a period of three months and they were observed visually and under an optical microscope and examined morphologically by TEM for the change in consistency and appearance of drug crystals upon storage. Also, Nano size, PDI and Zeta potential were examined [20]. The mean particle size of CSNPs loaded dispersion, surface charge (Zeta potential) and PDI was determined by using a Malvern zeta seizer (Malvern Instruments, UK) on the spot and monthly for three following months. The stability of nanoparticles to retain the drug was assessed, the retention of entrapped drug-loaded CSNPs formula was measured after preparation and then monthly of 3-mo duration [30]. Stability for the formulation was defined in terms of retaining its initial

entrapment efficiency for six months' duration. Stable formulation was defined by showing high entrapment efficiency (>60%) and high drug retention value (>90%) at each time interval, also non-significant change in size, PDI and Zeta potential.

Drug retained in CSNPs= Entrapped rivastigmine after storage/Entrapped rivastigmine before storage ×100.

RESULTS AND DISCUSSION

Preparation technique

Chitosan contains three functional groups; an amino group and primary and secondary hydroxyl groups at C2, C3 and C6 positions. The hydroxyl groups of chitosan make a chemical modification by attaching side groups to the reactive hydroxyl groups without altering its biophysical properties [31]. Chitosan nanoparticles CSNPs were first described in1994 by Ohya and co-workers. They used CSNPs prepared by emulsifying and crosslinking for intravenous delivery of anticancer drug 5-fluorouracil [32]. Since then, many methods have been employed for the syntheses of CSNPs. Five methods are presently available. They are ionotropic gelation, microemulsion, emulsification solvent diffusion, polyelectrolyte complex and reverse micellar method [33].

Ionotropic gelation technique was first reported by Calvo *et al.* [34] and has been widely examined and developed. The method utilizes the electrostatic interaction between the positively amine group of chitosan and a negatively charged group of polyanion such as tripolyphosphate. Nanoparticles were formed spontaneously under mechanical stirring at room temperature. The size and surface charge of particles can be modified by changing the ratio of chitosan to the stabilizer. Nanocapsules were formed as rivastigmine drug was in the core enclosed with polysaccharides shell which surrounded with surfactant. 25 plain CSNPs formulations were prepared using different ratios of Chitosan and TPP; through optimization processes, NPs with different diameters were obtained range from 229.8±11.10 nm to 783.3±29.20 nm. A general increase in particle compactness and size was observed on decreasing the chitosan concentration and on increasing the cross-linker to poly anion ratio [35]. Major optimization focused on lowering acetic acid concentration and ambient temperature. However, many other parameters were considered as the concentration of CS and TPP solution, pH, the temperature of the CS solution and stirring speed.

Ambient temperature during cross-linking plays an important role in forming high-quality NPs. Low ambient temperature was preferred because it causes a faster cooling rate of the dispersion, providing more hydrogen bond interaction between CS and water molecules. Not only that, at low ambient temperature, CS molecules stiffen faster and eventually stabilized the particles' structure [36]. Low molecular weight CS was used (50,000 Da) encapsulated rivastigmine more efficiently also pH plays a major role in the formulation of CSNPs. Nanoparticles like all the other kinds of Nano colloids, if injected in the bloodstream, are rapidly captured and destroyed by the reticuloendothelial system RES. To increase their half-life and, consequently, their activity, two strategies can be followed: to decrease their size [37] and/or to add a hydrophilic polymer or a surfactant (PEG, PS 80), different types of polysaccharides on their surface, which is capable of "masking" the NPs from the RES cells [11]. These hydrophilic molecules can be introduced on the surface of the NPs by adsorption or covalent bonding. The addition of a surfactant on the surface of the NPs also represents a suitable strategy to increase the passage of the BBB. In fact, it is demonstrated that the absence of the surfactant on the surface of the Nano colloids significantly decreases the transport of the particles to the CNS with, consequently, less pharmacological effect [38].

Many tests demonstrate that the passage across the BBB is due to receptor-mediated transcytosis. For example, in the case of PS 80-coated NPs, the surfactant placed on the surface of the Nano colloids is capable of interacting with the plasmatic LDLs and adsorbing them on their surface. Then, the LDL NPs can interact with the lipoprotein receptor expressed on the surface of the brain endothelial cells and, consequently, cross the BBB [39]. Moreover, it is demonstrated that the addition of PS 80 causes a rearrangement of the proteins that composed the TJs with a consequential increase in the Paracellular crossing of the NPs through the BBB [40]. Additionally, another proposed mechanism is that PS 80 plays a role in the blockage of the efflux system, reducing the pump-off effect of the P-gp, and consequently, a higher pharmaceutical drug concentration in the brain is achieved. PS 80-coated NPs are used to facilitate transport through the BBB of different kinds of pharmaceutical drugs.

Table 1: Composition, particle size, polydispersity and Zeta potential analysis data of 25 plain chitosan nanoparticles formulations; (n=3)

Formula code	Composition		Particle size (nm)	PDI	Zeta potential (mV)
	Chitosan %w/v	Sodium TPP %w/v			
F1	0.5	1.4	783.3±29.20	0.570±0.023	25.6±1.13
F2	0.7	1.4	521.5±64.13	0.596±0.098	22.9±0.495
F3	1	1.4	486.4±27.22	0.363±0.031	38.0±0.283
F4	1.2	1.4	339.1±54.09	0.452±0.016	22.1±0.070
F5	1.4	1.4	289.6±4.525	0.356±0.005	23.5±0.070
F6	0.5	1.2	456.3±18.31	0.403±0.035	17.8±1.77
F7	0.7	1.2	549.2±10.61	0.447±0.035	13.5±0.424
F8	1	1.2	599.7±0.503	0.000	16.6±0.141
F9	1.2	1.2	267.5±2.475	0.376±0.045	24.0±2.26
F10	1.4	1.2	236.9±18.03	0.370±0.011	22.5±2.33
F11	0.5	1	395.3±26.23	0.417±0.013	21.0±1.27
F12	0.7	1	321.0±40.38	0.384±0.069	22.9±0.141
F13	1	1	288.0±0.495	0.333±0.04	20.1±0.566
F14	1.2	1	412.5±17.04	0.409±0.017	23.5±0.283
F15	1.4	1	229.8±11.10	0.361±0.001	26.5±1.56
F16	0.5	0.8	364.6±15.19	0.309±0.001	20.3±3.54
F17	0.7	0.8	371.3±24.04	0.374±0.007	26.3±0.566
F18	1	0.8	322.8±28.92	0.419±0.038	24.5±0.566
F19	1.2	0.8	298.2±4.384	0.347±0.032	26.3±0.495
F20	1.4	0.8	280.1±49.14	0.377±0.023	27.6±0.495
F21	0.5	0.6	238.3±39.81	0.518±0.032	31.0±0.495
F22	0.7	0.6	395.3±6.152	0.424±0.054	29.0±0.778
F23	1	0.6	351.0±21.92	0.475±0.033	29.9±1.84
F24	1.2	0.6	308.0±9.617	0.428±0.010	30.3±1.06
F25	1.4	0.6	372.6±40.87	0.447±0.134	29.9±2.97

n= number of determination; mean±Standard Deviation

Particle size analysis

25 different formulas of plain CSNPs with the same final dispersion volume were used to see the changes on size, polydispersity and surface charge potential with different chitosan and cross-linker ratios. Refer to table 1 and fig. 2 (A, B andC). The incorporation of two compounds with different concentrations ratios into CNPs will affect the particle size also polydispersity. It was noticed that particle size was decreased significantly by decreasing the ratio between CS and cross-linker from 0.5:1.4 to 1.4:0.6 %w/v, as shown in table 1 with decrease cross-linker concentration and increase CS. This phenomenon was expected as lower viscosity of CS lower molecular weight resulted in a better solubility and subsequently, better interaction between CS and cross-linkers, and thus, produced smaller particle size [36, 41]. The optimum formula F15 was chosen with particle size 229.8 d. nm, PDI 0.361 and zeta potential was 26.5 mV after application of desirability factor equation relative to targeted and maximum Nano size, lower PDI and higher zeta potential and value with total desirability near 1 was chosen, as for the PDI, the lowest was 0.309±0.001 and the highest was 0.596±0.098, shown by formulations F 16 and F2 respectively. Higher PDI indicates that the sample might have agglomerated; this is possible because CS is very sensitive to water, which can cause it to easily form lumps. Table 2 showed the optimum formula loaded with different drug concentrations; the larger loaded chitosan Nano particles obtained was 490.6±7.425 nm with the highest RS concentration 4 %w/v, entrapment efficiency % was 89.802 and drug loading was 40.81%. Zeta potential is identified with the charge on the surface of the molecule, thus impacts an extensive range of properties of colloidal materials, for example, their stability, interaction with electrolytes and suspension rheology. Literature suggested that zeta potential value should lie in the range of-20 mV to+30 mV. Zeta potential was found to be ranged from 16.6±0.141mV to 31.0±0.495 mV that indicates the formation of a stable formulation. In general, positive Zeta potential values of CSNPs due to carboxyl group of chitosan.

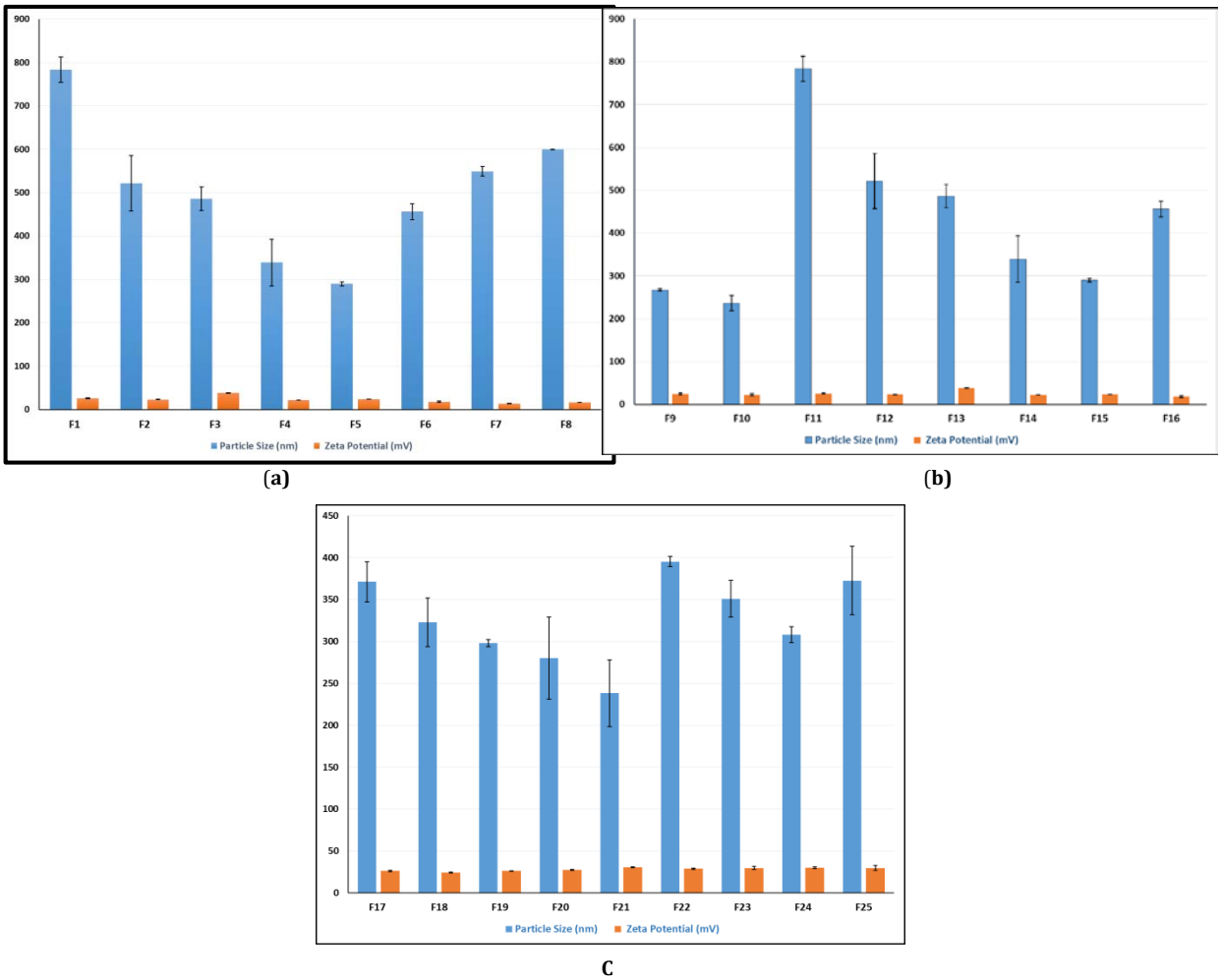

Fig. 2: (a F1-F8, b F9-F16 and cF17-F25) Effect of chitosan and cross-linker different ratios on particle size and zeta potential of 25 plain CSNPs formulations

Table 2: Effect of different rivastigmine concentrations loaded in optimum CSNPs (F15) on physical and chemical characterizations; (n=3)

Rivastigmine (%w/v)	Particle size (nm)	PDI	Zeta potential (mV)	Entrapment efficiency %	Drug loading %
0.5	291.6±7.707	0.329±0.002	29.0±0.636	71.59	6.75
1	245.1±11.88	0.306±0.026	25.0±0.212	83.77	14.44
2	257.0±20.44	0.370±0.029	25.0±0.707	85.58	25.17
3	243.6±4.031	0.224±0.000	24.6±0.566	87.41	33.62
4	490.6±7.425	0.450±0.014	23.0±0.919	89.802	40.81

n= number of determination; mean±Standard Deviation

Morphology of Rivastigmine loaded optimal formula by optical and electron microscopy

Fig. 3 shows the morphology of nanoparticles by optical microscopy, the particles are smooth circular, encapsulating drug in the core and all particles are approximately in the same size. Particles surface surrounded with thin layer of non-ionic surfactant tween 80 assure particle stability and enhance uptake by cells. Fig. 4 (A) and (B) show TEM morphology of nanoparticles in aqueous dispersion at 40,000 magnifications, the largest particles were found in drug-loaded CSNPs through range from 31.7 d. nm to 115 d. nm while unloaded CSNPs were smaller in size range from 9.73 d. nm to 50.5 d. nm. Fig. 5 shows SEM the particles appear spherical with a hairy surface.

Percentage drug content

Optimum formula F15 was loaded with 4% w/v RS showed high percentage drug content reached to 98.93%. The predominant influencing factors could be good percent entrapment efficiency, narrow Nano size scale distribution of the colloidal dispersion also nanoparticles were fairly stable.

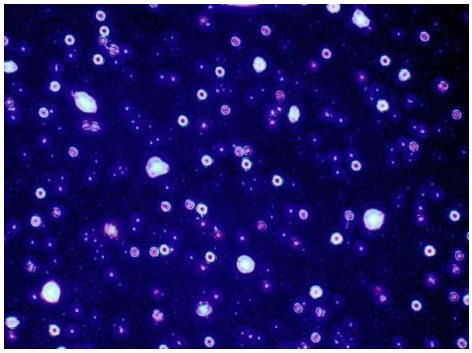

Fig. 3: Optical view of loaded optimum CSNPs formula (F15)

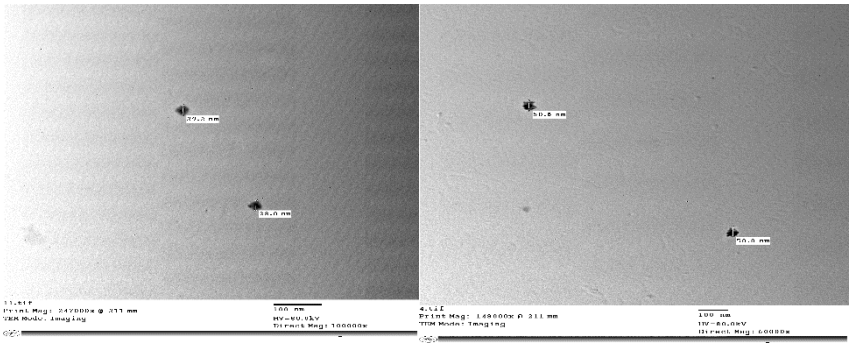

(a) **(b)**

Fig. 4: (a) TEM image of plain and (b) drug loaded CSNPs optimum formula (F15)

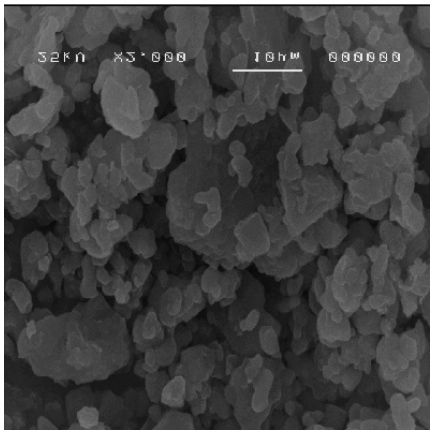

Fig. 5: SEM image of drug-loaded CSNPs optimum formula (F15)

Entrapment efficiency and drug loading

Entrapment efficiency was studied for five different RS concentrations (0.5% w/v, 1% w/v, 2% w/v, 3% w/v and 4% w/v) loaded in optimum formulas F15. As shown in table 2 the EE % was increased as the drug concentration increased 71.59%, 83.77%, 85.58%, 87.41% and 89.802% respectively. Formula which gave highest EE % (89.802%) loaded with 4% w/v RS was chosen for further studies including ex-vivo release study.

Thermal analysis (DSC)

Depicts the DSC curves for commercial purified chitosan, DA = 15.9%, at different heating rates. Fig. 6 shows all curves, an endothermic peak at 28.96 °C can be ascribed to the loss of water and dehydration. Glass transition temperature of chitosan at 61.1 °C as the glass transition temperature is the change in sample heat capacity. This confirms that water does acts as a plasticizer in chitosan. Water form an intermolecular hydrogen bonding with chitosan through amine and hydroxyl groups present in them. This helps in molecular rearrangement, which eases the chain mobility in chitosan. Two exothermic peaks are observed at 286.80 and 307.50 °C related to the thermal decomposition for amine (GlcN) and acetyl (GlcNAc) residues, respectively, characteristic for chitosan sample. Thus, the amine residues are thermally less stable than acetyl ones; these results were inconsistent with Prerna *et al.* [42]. STPP have melting temperature at 54.18 °C was shown by endothermic peak. Clear glass transition

endothermic peak was observed at 73.38 °C. RS exhibited a sharp peak at 217.89 °C due to the anhydrous crystal form of the drug, onsite of melt at a 107.77 °C, melting point at 125.37 °C and completion of melt at 127.34 °C also RS demonstrated an endothermic phase transition at 69.28 °C. The physical mixture shows similar peaks support physical compatibility except that RS endothermic sharp peak shift to 231.52 °C. The formula of nanoparticles clarify the disappearance of most previous peaks and appear of new sharp endothermic peak at 63.64 °C, RS peak shift to 321.21 °C provided the evidence of a reduction in crystallinity and increase in hydrophobicity or amorphous state.

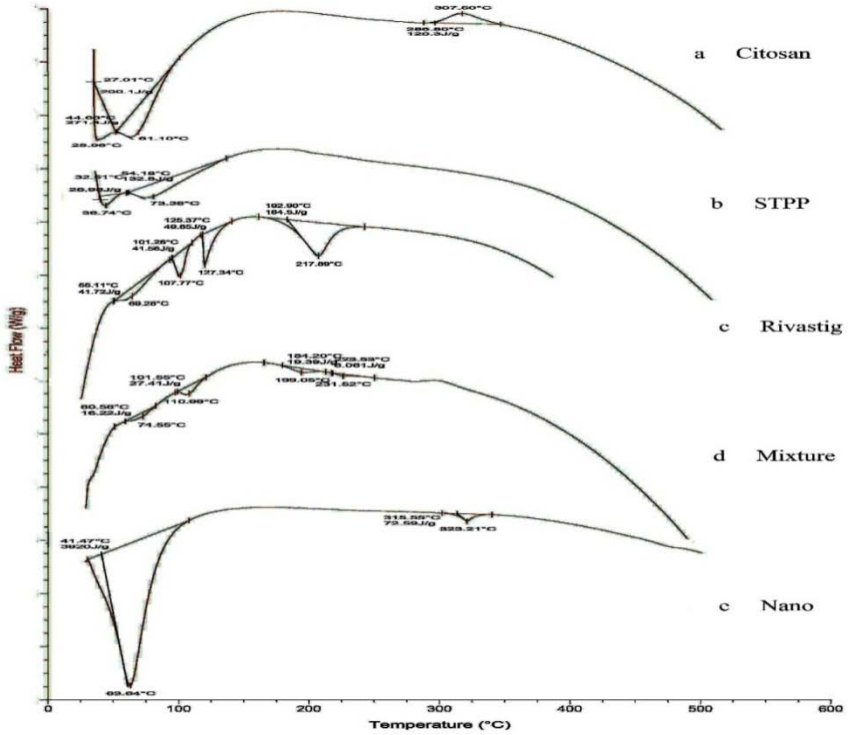

Fig. 6: DSC Thermogram of (a) chitosan, (b) STPP, (c) rivastigmine, (d) Physical mixture and (e) optimum loaded CSNPs formula respectively

Rheology study

As shown in fig. 7, demonstrating thixotropic (shear-thinning) properties; There were a correlation between shear stress and shear rate. When the shear rate of Nano-gel was increased (up curve), shear stress was also increased with yield value, indicating pseudo plastic (non-Newtonian) behavior and viscosity decreased with increasing shear rate and shear stress. Viscosity decreases with increase in shear rate (rubbing action means increased shear rates and stress); while viscosity regains after shearing stops. This is called 'Thixotropic'. As Farrow's constant is greater than one; it indicates pseudoplastic or plastic flow and contributes to good flow characteristics and favorable spreadability upon topical application [43]. Rheological properties such as viscosity and thixotropic of semi-solid dosage forms can influence their drug delivery. Viscosity may directly influence the diffusion rate of the drug.

Therefore, the product flow behavior must be monitored at the time of its application. This also helps to monitor batch-to-batch consistency. Most topical semisolids, when applied on the surface of the skin, show non-Newtonian behavior. The structures formed within semisolid drug products during manufacturing can show a wide range of behaviors, including shear thinning, viscosity, thixotropic and irreversible or reversible structure damage.

Brookfield R/S Cone Plate Rheometer with CFR 21 compliance is a good option to measure viscosity and rheology of topical semisolids.

A number of rheological properties play an important role in determining how a material behaves as it moves from storage to handling environment and vice-versa. For example, the force or stress required to initiate flow (yield point) of fluids and semi-solid products plays a significant role in the shelf-life, storage, transfer, packaging and end-use performance of those materials.

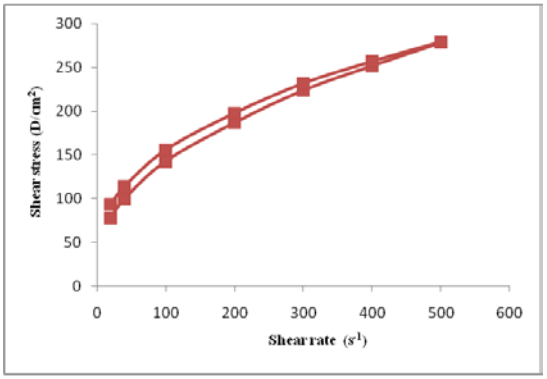

Fig. 7: Shear stress versus shear rate indicates thixotropic (shear-thinning) flow of loaded optimum formula CSNPs gel

Skin irritancy test

The selected optimum loaded gel formulation (F15) showed no irritation potential, thus proving to be non-irritant as it was mentioned by Van-Abbé *et al.* [26], that a value between 0 and 9 in an irritancy test indicates that the applied formulation is generally non-irritant to human skin. No obvious erythema, edema or inflammation was observed on mice' skin after one week of application of the selected formulas compared to the control area.

Ex-vivo drug release studies

Three different RS formulas were ex-vivo release studied containing the same RS concentration 4% w/v, drug solution, aqueous

dispersion and optimized batch of the RS loaded chitosan nanoparticles gel using mice skin and Franz diffusion cells and was repeated thrice, mean±SD shown in table 3 and fig. 8. In this formulation system, the release of the drug was found to be nearly complete and the formulations tested showed a biphasic release pattern: one initial fast release followed by a second slow release phase (extended-release). The burst effect could be attributed to the escape of the drug from the surface of the polymeric system because the drug present in the polymeric matrix diffuses to the release medium through the pores and channels of the polymeric nanoparticles. The kind of polymer also affected drug release behavior, as the chitosan polymer was found to be more hydrophilic by the aid of glacial acetic acid and amorphous; these properties were also responsible for the biphasic release pattern. Furthermore, the homogenous and finer dispersion of the drug molecules in the polymer matrix enhances the dissolution allowing the better penetration of the dissolution medium through the nanoparticles. The dispersion of RS in the polymer matrices led to a gradual dissolution and release of the drug, which will be complete over 24 h.

Table 3: Percent release of rivastigmine CSNPs gel formula, Nano dispersion and aqueous solution; (n=3)

Time (h)	Nano gel	Nano dispersion	Solution
1	26.018±3.01	10±5.01	14.23±5.92
2	29.498±5.22	21±4.83	21.273±5.86
4	50.297±4.11	29.261±3.65	29.102±4.60
8	54.33±3.52	40.056±5.53	30.605±5.11
12	71.096±7.02	46±6.65	34.006±6.00
16	79.004±6.31	50.404±7.11	53±6.31
18	74±5.81	46.105±5.64	32.294±5.74
20	71.175±4.74	37.05±4.03	19.05±5.62
24	71±3.76	34±4.44	12.268±5.00

n= number of determination; mean±Standard Deviation

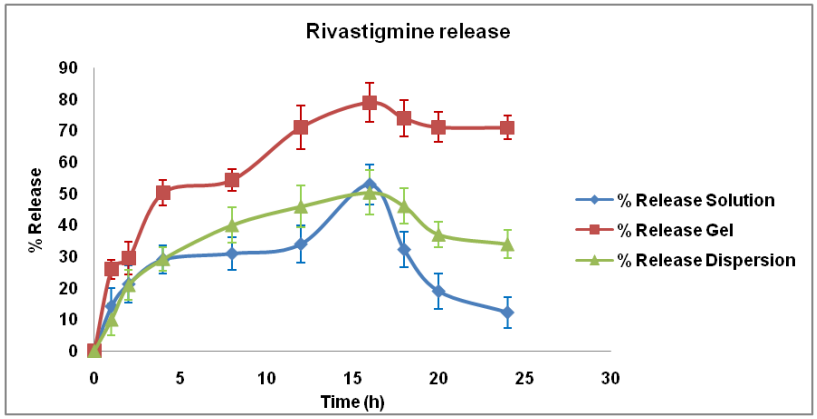

Fig. 8: mean±SD % release of rivastigmine from CSNPs gel, aqueous nano dispersion and aqueous solution loaded with 4 %w/v drug. (n=3); n= number of determination

Permeation of nano-gel

All the epidermis and the hair are covered by negative charges as cellular surface is dominated by negatively charged sulphated proteoglycans and phosphatidylcholine molecules that play pivotal roles in cellular proliferation, migration and motility. However, these charges are often covered by a neutral lipid film. Electrostatic attraction between CSNPs carried positive charge and skin surface in addition to the ability of the CSNPs coated with tween 80 to penetrate into intercellular regions, disordering and fluidizing the intercellular lipid lattices in the stratum corneum, might be related to the enhancing effect of the transdermal permeation surfactants [44].

The fluidity of the stratum corneum lipids i.e. soften and swell by the CSNPs formulae without serious structural changes of the skin suggest interruption of the stratum corneum lipids by the loaded CSNPs also improved RS flux and permeation. With 0.5 w/v carbopol, the gel viscosity was increased due to cross-linking of the polymer chain network and skin bioadhesive ability furthermore the initial aqueous media of gel facilitate attraction of loaded Nano-gel into deeper water trigger skin layer reach with blood capillaries'. As result RS systemic blood absorption from Nano-gel was better than non-skin adhesive CSNPs aqueous dispersion. Depending on the drug the skin permeability's are in the range 0.01–10 µg of drug/cm^2· h, drugs delivered through the skin must be effective at doses of 0.01 mg/d for a poorly skin-permeable drug and 10 mg/d for a highly skin-permeable drug.

RS is a small molecule (400 Da), and is both hydrophilic and lipophilic. These properties beside optimum formulae F15 loaded with RS concentration 4% w/v equivalent to 20 mg/g gel containing penetration enhancement surfactant may spread on 25 cm^2 skin area refers that RS can pass easily through the skin into bloodstream as well as through blood-brain barrier making it well-suited to brain through transdermal delivery.

Kinetic behavior

The data of the release of the RS from the Nano gel were fitted to six kinetic models, which are described as shown in table 4. The result indicated that the release of the drug from the Nano gel followed the diffusion kinetic model, with the best fit value for the correlation coefficient (R^2) at 0.9343 as shown in fig. 9. The rate of drug release from any solid or semi-solid delivery system is usually controlled by dissolution and/or diffusion. Regardless of mechanisms involved in the release, its rate under sink conditions can be expressed by a single general equation as follows:

$$dw/dt = D/h. SCs$$

W is amount of drug released up to time t and dw/dt is the rate of release. D, S, Cs and h are drug molecule diffusion coefficient, effective surface area of drug with release medium, drug solubility in the medium and the length of diffusion path. This equation represents both the Noyes-Whitney law of dissolution [45], applied for dissolution rate-limited release as well as the Fick's first law for

diffusion rate-limited release processes [46]. In the dissolution process h, the thickness of the stagnant aqueous layer around drug particle is constant but S and sometimes D are varied during the release process [47]. On the other hand, in a diffusion rate, limited release in addition to D, h and sometimes S are variable during the release process. For a complex system such as nanoparticles the previous equation does not seem to include all other factors influencing the release rate among which penetration rate of liquid into the system; hydration, swelling, relaxation, erosion and dissolution of polymer can be mentioned. The extents of liquid penetration and the polymer contributed properties are directly proportional to $t_{1/2}$ and powered of t, respectively. Thus, these effects are collectively represented as time-dependent variable, X, and the equation becomes:

$$Dw/dt = D/h. SCs X$$

Therefore, regardless of a release mechanism in order to obtain a general working formula for both dissolution and diffusion rate-limited release processes it is assumed that the term DSX/h is variable during the release.

Table 4: Data fitting for rivastigmine release from the CSNPs gel were fitted to six kinetic models

Models	Zero	First	Second	Diffusion	Hixon	Baker	Chosen "r"
a	34.40117	1.817007	0.015089	17.29466	0.609421	0.024041	
b	0.03441	-0.00034	1.96E-05	1.690043	0.000917	0.000106	
r	0.874962	-0.87189	0.834049	0.934324	0.876516	0.87058	0.934324
k	0.03441	-0.00079	1.96E-05	1.690043	0.000917	0.000106	
t(1/2)	1453.049	-877.946	509.0386	875.2753	1042.172	521.0195	

r; Coefficient of determination value

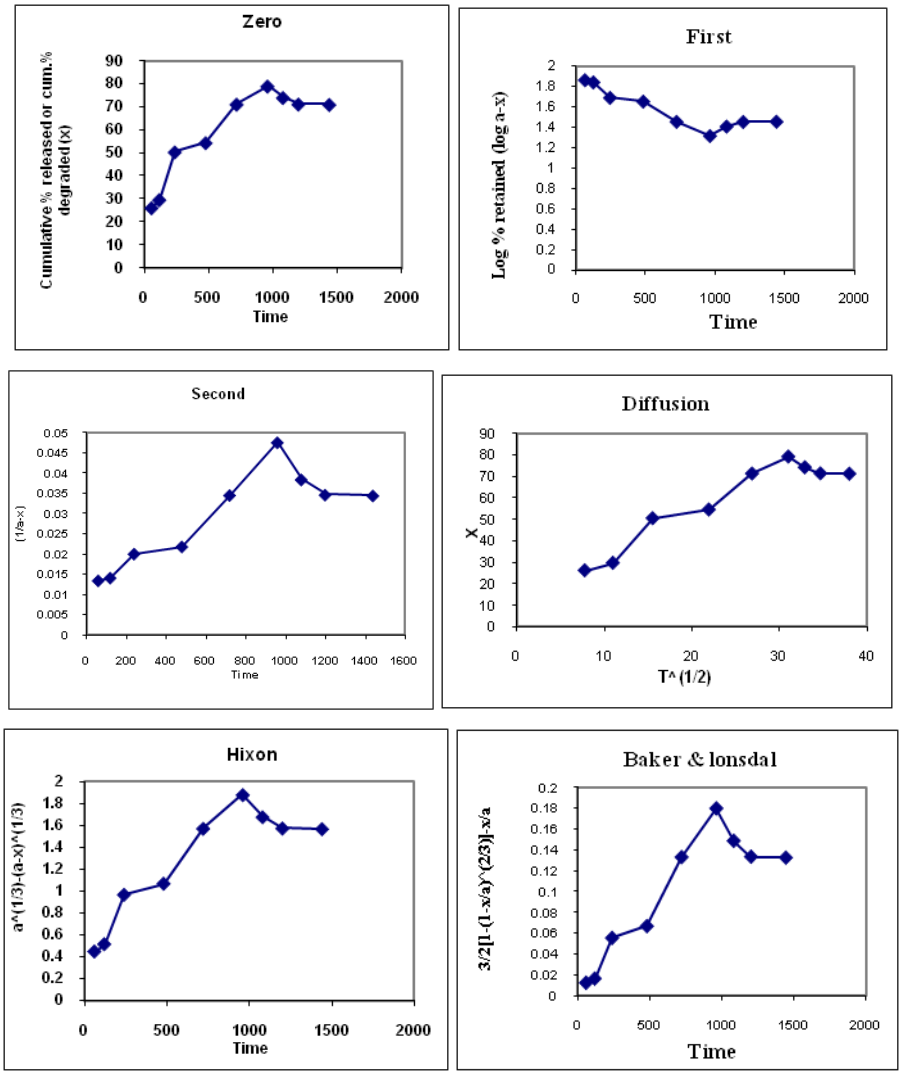

Fig. 9: Rivastigmine CSNPs gel follow diffusion drug release kinetic model

Stability of loaded optimum formula

Table 5 clarify the three-mo stability study of the optimized loaded formula measured monthly at two different temperatures. The average Nano size at 25 °C was 373.8±11.5 nm, and that at 4 °C was 433.73±12.58 nm. The PDI was about 0.4 and no significant change in Zeta potential. The average Nano size measured by TEM was 25±15. Indicating stable CSNPs carriers especially stored at low temperature.

Three mo tested loaded formula showed no significant difference in Zeta Potential (mV), Entrapment Efficiency%, Drug Loading % and Drug retention % was 100%. These results emphasize that loaded CSNPs carriers are fairly stable over a three-mo stability study.

Table 5: Three mo physicochemical stability study of optimum loaded nanodispersions (F15) at 4 °C and ambient room temperature; (n=3)

At 4 °C	Particle size (nm)	PDI	Zeta potential (mV)	Entrapment efficiency %	Drug loading %	Drug retention %
On the spot	429.5±23.83	0.375±0.042	23.2±0.424	88.46	40.290	
Mo 1	450.5±25.12	0.355±0.031	23.00±0.515	88.415	40.188	100
Mo 2	430.7±30.51	0.352±0.0245	23.67±0.760	88.215	40.245	100
Mo 3	420±36.90	0.315±0.045	23.11±0.532	88.00	40.11	100
At room temperature	Particle size (nm)	PDI	Zeta potential (mV)	Entrapment efficiency%	Drug loading %	Drug retention %
On the spot	354.6±14.78	0.440±0.042	26.0±0.778	88.491	40.223	
Mo 1	380.8±20.11	0.465±0.127	23.2±0.566	90.405	41.093	100
Mo 2	360.5±45.00	0.400±0.043	24.8±0.911	89.00	40.18	100
Mo 3	380.2±55.13	0.465±0.065	25.9±0.76	89.12	40.00	100

n= number of determination; mean±Standard Deviation

CONCLUSION

Rivastigmine-loaded nanoparticles were prepared successfully using the ionic gelation method modified by in the presence of polysorbate 80 as a surfactant and stabilizer. This method was found to be simple and produced nanoparticles with a narrow size distribution and acceptable entrapment efficiency and drug loading. The particle size and drug entrapment were optimized based on the study of the effect of different formulation variables. A change in the concentration of the, polymer, crosslinker and rivastigmine concentration was found to vary the size, polydispersity index, zeta potential and entrapment efficiency of the prepared nanoparticles. The effect of different formulation variables helped in the optimization of the formulation in achieving higher efficacy and drug loading. Rivastigmine-loaded CSNPs was not skin irritant. The *Ex vivo* release study revealed sustained release of rivastigmine loaded CSNPs gel for 24 h, the best release pattern was observed in Nano gel formula followed by Nano dispersion as bioadhesive naturally polymer Nano gel and non-ionic surfactant coat enhance skin permeation, systemic absorption and cross blood brain barrier. Percentage drug release data of best formulation F15 fitted in diffusion plot which was indicative of a present diffusion work was fulfilled by formulating rivastigmine polymeric nanoparticles for passive targeting of brain-controlled drug delivery system there by increasing timed release of drug. The chosen optimum formula was physical and chemical stable at different temperature along three mo.

ACKNOWLEDGEMENT

The authors are thankful for Mach Premiere Pharmaceutical Industries in Egypt for gift of pure Rivastigmine drug, also for research lab of Future University in Egypt.

FUNDING

The authors did not receive any funding for this research work.

AUTHORS CONTRIBUTIONS

The experiment was conducted under the guidance of Mona Ibrahim: conduct of experiments design and work, literature collection, and analysis, Dalia Samuel: Provided facilities for the experiments, writing revision.

CONFLICT OF INTERESTS

The authors declare that there is no conflict of interest.

REFERENCES

1. Chakraborty C, Sarkar B, Hsu CH, Wen ZH, Lin CS, Shieh PC. Future prospects of nanoparticles on brain targeted drug delivery. J Neurooncol. 2009;93(2):285-6. doi: 10.1007/s11060-008-9759-2, PMID 19048187.
2. Chen Y, Dalwadi G, Benson HAE. Drug delivery across the blood-brain barrier. Curr Drug Deliv. 2004;1(4):361-76. doi: 10.2174/1567201043334542, PMID 16305398.
3. Pasha K, Imtiyaz A. Evaluation of anti-alzheimer activity of alcoholic extract of *Costus pictus* D. Don leaves in wistar albino rats. Asian J Pharm Clin Res. 2020;13(2):36-43.
4. Saha P, Goyal AK, Rath G. Formulation and evaluation of cgitosan-based ampicillin trihydrate nanoparticles. Trop J Pharm Res. 2010;9(5):483-8.
5. Modi G, Pillay V, Choonara YE, Ndesendo VMK, du Toit LC, Naidoo D. Nanotechnological applications for the treatment of neurodegenerative disorders. Prog Neurobiol. 2009;88(4):272-85. doi: 10.1016/j.pneurobio.2009.05.002, PMID 19486920.
6. Dustgani A, Farahani EV, Imani M. Preparation of chitosan nanoparticles loaded by dexamethasone sodium phosphate. Iran J Pharm Sci. 2008;4(2):111-4.
7. Hughes GA. Nanostructure–mediated drug delivery. Nanomedicine. 2005;1(1):22-30. doi: 10.1016/j.nano.2004.11.009, PMID 17292054.
8. Craparo EF, Pitarresi G, Bondì ML, Casaletto MP, Licciardi M, Giammona G. A nanoparticulate drug-delivery system for rivastigmine: Physico-chemical and in vitro biological characterization. Macromol Biosci. 2008;8(3):247-59. doi: 10.1002/mabi.200700165, PMID 18041108.
9. Singh R, Lillard JW. Nanoparticle-based targeted drug delivery. Exp Mol Pathol. 2009;86(3):215-23. doi: 10.1016/j.yexmp.2008.12.004, PMID 19186176.
10. Lockman PR, Koziara JM, Mumper RJ, Allen DD. Nanoparticle surface charges alter blood-brain barrier integrity and permeability. J Drug Target. 2004;12(9-10):635-41. doi: 10.1080/10611860400015936, PMID 15621689.
11. Kreuter J. Nanoparticulate systems for brain delivery of drugs. Adv Drug Deliv Rev. 2001;47(1):65-81. doi: 10.1016/s0169-409x(00)00122-8, PMID 11251246.
12. Meena M, Zehra A, Swapnil P, Harish, Marwal A, Yadav G, Sonigra P. Endophytic nanotechnology: an approach to study scope and potential applications. Front Chem. 2021;9:613343. doi: 10.3389/fchem.2021.613343. PMID 34113600.
13. Malhotra M, Kulamarva A, Sebak S, Paul A, Bhathena J, Mirzaei M, Prakash S. Ultrafine chitosan nanoparticles as an efficient nucleic acid delivery system targeting neuronal cells. Drug Dev Ind Pharm. 2009;35(6):719-26. doi: 10.1080/03639040802526789, PMID 19514987.
14. Tekin S, Lane R. Rivastigmine in the treatment of dementia associated with parkinson's disease: a randomized, double-blind, placebo-controlled study. Prog Neurother Neuropsychopharmacol. 2006;1(1):13-25. doi: 10.1017/S1748232105000030.
15. Kaur P, Rao R, Hussain A, Khatkar S. Preparation and characterization of rivastigmine loaded chitosan nanoparticles. J Pharm Sci Res. 2011;3(5):1227-32.

16. Mukhopadhyay S, Madhav NV, Upadhyaya K. Formulation and evaluation of bio-nanoparticulated drug delivery of rivastigmine. World J Pharm Sci. 2016;4(5):264-72.
17. Manek E, Darvas F, Petroianu GA. Use of biodegradable, chitosan-based nanoparticles in the treatment of Alzheimer's diease. Molecules. 2020;25(4866):1-26.
18. Zynopsicha Armatazaka, TN Saifullah Sulaiman, Zulkarnain AK. Optimization and characterization of PEG-PCL-PEG triblock copolymer as carrier of drug-using full factorial design. Int J Curr Pharm Sci 2019;11(5):65-71. doi: 10.22159/ijcpr.2019v11i5.35706.
19. Liu C, Tan Y, Liu C, Chen X, Yu L. Preparations, characterizations and applications of chitosan–based nanoparticles. J Ocean Univ China. 2007;6(3):237-43. doi: 10.1007/s11802-007-0237-9.
20. Mokhtar M, Sammour OA, Hammad MA, Megrab NA. Effect of some formulation parameters on flurbiprofen encapsulation and release rates of niosomes prepared from proniosomes. Int J Pharm. 2008;361(1-2):104-11. doi: 10.1016/j.ijpharm.2008.05.031, PMID 18577437.
21. Cho EJ, Holback H, Liu KC, Abouelmagd SA, Park J, Yeo Y. Nanoparticle characterization: state of the art, challenges, and emerging technologies. Mol Pharm. 2013;10(6):2093-110. doi: 10.1021/mp300697h, PMID 23461379.
22. Hu CJ, Rhodes DG. Proniosomes: a novel drug carrier preparation. Int J Pharm. 1999;185(1):23-35. doi: 10.1016/s0378-5173(99)00122-2, PMID 10425362.
23. Yadav SK. Nanoscale materials in targeted drug delivery, theragnosis and tissue regeneration. New York: Springer; 2016.
24. Uppuluru AK, Gande S. Preparation and *in vivo* evaluation of candesartan cilexetil solid dispersions. Asian J Pharm Clin Res. 2021;14(8):129-33.
25. Chaitali S, Ruchi S, Ananya B, Srinivas P, Superiya S. Formulation and QBD optimization of methotrexate-loaded solid lipid nanoparticles for an effective anti-cancer treatment. Int J Appl Pharm. 2021;13(5):132-43.
26. Van-Abbe NJ, Nicholas P, Boon E. Exaggerated exposure in topical irritancy and sensitization testing. J Soc Cosmet Chem. 1975;26:173.
27. Nair VB, Panchagnula R. The effect of pretreatment with terpenes on transdermal iontophoretic delivery of arginine vasopressin. Farmaco. 2004;59(7):575-81. doi: 10.1016/j.farmac.2004.02.004, PMID 15231435.
28. Vashisth I, Ahad A, Aqil M, Agarwal SP. Investigating the potential of essential oils as penetration enhancer for transdermal losartan delivery: effectiveness and mechanism of action. Asian J Pharm Sci. 2014;9(5):260-7. doi: 10.1016/j.ajps.2014.06.007.
29. Pourjavadi A, Barzegar S, Mahdavinia GR. MBA-crosslinked Na-Alg/CMC as smart full-polysaccharide superabsorbent hydrogels. Carbohydr Polym. 2006;66(3):386-95. doi: 10.1016/j.carbpol.2006.03.013.
30. Pardakhty A, Varshosaz J, Rouholamini A. *In vitro* study of polyoxyethylene alkyl ether niosomes for delivery of insulin. Int J Pharm. 2007;328(2):130-41. doi: 10.1016/j.ijpharm.2006.08.002, PMID 16997517.
31. Rajasree R, Rahate K. An overview on various modifications of chitosan and its applications. Int J Pharm Sci Res. 2013;4(11):4175-93.
32. Grenha A. Chitosan nanoparticles: a survey of preparation methods. J Drug Target. 2012;20(4):291-300. doi: 10.3109/1061186X.2011.654121, PMID 22296336.
33. Tiyaboonchai W. Chitosan nanoparticles: a promising system for drug delivery. Naresuan Univ J. 2003;11(3):51-66.
34. Calvo P, Remunanaen-Lopez C, Vila Jato JL, Alonso MJ. Novel hydrophilic chitosan-polyethylene oxide nanoparticles as protein carriers. J Appl Polym Sci. 1997;63(1):125-32. doi: 10.1002/(SICI)1097-4628(19970103)63:1<125:AID-APP13>3.0.CO;2-4.
35. Jonassen H, Kjøniksen AL, Hiorth M. Stability of chitosan nanoparticles cross-linked with tripolyphosphate. Biomacromolecules. 2012;13(11):3747-56. doi: 10.1021/bm301207a, PMID 23046433.
36. Fan W, Yan W, Xu Z, Ni H. Formation mechanism of monodisperse, low molecular weight chitosan nanoparticles by ionic gelation technique. Colloids Surf B Biointerfaces. 2012;90:21-7. doi: 10.1016/j.colsurfb.2011.09.042, PMID 22014934.
37. Nguyen TV, Nguyen TTH, Wang SL, Vo TPK, Nguyen AD. Preparation of chitosan nanoparticles by TPP ionic gelation combined with spray drying, and the antibacterial activity of chitosan nanoparticles and a chitosan nanoparticle–amoxicillin complex. Res Chem Intermed. 2017;43(6):3527-37. doi: 10.1007/s11164-016-2428-8.
38. Alam S, Khan ZI, Mustafa G, Kumar M, Islam F, Bhatnagar A, Ahmad FJ. Development and evaluation of thymoquinone-encapsulated chitosan nanoparticles for nose-to-brain targeting: a pharmacoscintigraphic study. Int J Nanomedicine. 2012;7:5705-18. doi: 10.2147/IJN.S35329, PMID 23180965.
39. Allen DD, Smith QR. Characterization of the blood-brain barrier choline transporter using the in situ rat brain perfusion technique. J Neurochem. 2001;76(4):1032-41. doi: 10.1046/j.1471-4159.2001.00093.x, PMID 11181822.
40. Zhang Y, Pardridge WM. Rapid transferrin efflux from brain to blood across the blood-brain barrier. J Neurochem. 2001;76(5):1597-600. doi: 10.1046/j.1471-4159.2001.00222.x, PMID 11238745.
41. Raja MA, Katas H, Jing Wen T. Stability, intracellular delivery, and release of siRNA from chitosan nanoparticles using different cross-linkers. PLOS ONE. 2015;10(6):e0128963. doi: 10.1371/journal.pone.0128963. PMID 26068222.
42. Dhawade PP, Ramanand N. Characterization of the glass transition temperature of chitosan and its oligomers by temperature modulated differential scanning calorimetry. Adv Appl Sci Res. 2012;3(3):1372-82.
43. Helal DA, El-Rhman DA, Abdel-Halim SA. Formulation and evaluation of fluconazole topical gel. Int J Pharm Pharm Sci. 2012;4:176-83.
44. Obata Y, Utsumi S, Watanabe H, Suda M, Tokudome Y, Otsuka M, Takayama K. Infrared spectroscopic study of lipid interaction in stratum corneum treated with transdermal absorption enhancers. Int J Pharm. 2010;389(1-2):18-23. doi: 10.1016/j.ijpharm.2010.01.007, PMID 20079819.
45. Noyes AA, Whitney WR. The rate of solution of solid substances in their own solutions. J Am Chem Soc. 1897;19(12):930-4. doi: 10.1021/ja02086a003.
46. Higuchi T. Mechanism of sustained-action medication theoretical analysis of rate of release of solid drugs dispersed in solid matrices. J Pharm Sci. 1963;52:1145-9. doi: 10.1002/jps.2600521210, PMID 14088963.
47. Macheras P, Dokoumetzidis A. On the heterogeneity of drug dissolution and release. Pharm Res. 2000;17(2):108-12. doi: 10.1023/a:1007596709657, PMID 10751023.